Point-Defects-Induced Vortex Phase Diagram in High-T_c Superconductors: Monte Carlo Simulation Study

Ryoko Sugano [a], Toshiyuki Onogi [a], Kazuto Hirata [b] Masashi Tachiki [b]

[a] *Advanced Research Laboratory, Hitachi, Ltd., Hatoyama, Saitama 350-0395, Japan*

[b] *National Institute for Materials Science, 1-2-1 Sengen, Tsukuba, Ibaraki 305-0047, Japan*

Abstract

We investigated the vortex phase diagram of high-T_c copper-oxide superconductors in the presence of dense point defects (PDs), by using a Monte Carlo simulation based on the Lawrence-Doniach model. We found a temperature-driven depinning line within the Bragg and vortex glass phases, well below the melting line in the case of high anisotropy. We also found a field-driven transition line from the Bragg-to-vortex glass at low temperatures, accompanied by an abrupt reduction in the interlayer vortex correlation. The complex phase boundaries are drastically controlled by the pinning force of PDs, defect density, and anisotropy.

Key words: vortex phase diagram, copper-oxide superconductors, point defects,Monte Carlo simulation

In the high-T_c copper-oxides, a vortex state exhibits drastic dependence on anisotropy, carrier doping, and inhomogeneity inherent in a single crystal. In particular, randomly distributed pointlike defects (PDs), act as not only individual pinning centers but also promoters of the vortex-line wandering along the c-axis. Possible vortex-matter phases are then expected to become complicated [1]. In our previous Monte Carlo simulation[2], we numerically presented a field(B)-temperature(T) vortex phase diagram of a $Bi_2Sr_2CaCu_2O_{8+\delta}$(BSCCO) model intrinsic to randomly distributed PDs. The obtained phase diagram consists of three principal phases: Bragg glass(BG), vortex glass(VG), and pancake gas(PG). We also found a depinning line well below the melting line.

In this paper, focusing on the effects of anisotropy, we make a comparative study of the vortex phase diagram in the presence of densely distributed PDs, based on the Lawrence-Doniach model. We have performed the Monte Carlo simulation with N_v vortex-lines penetrating through N_z layers in the presence of PDs at finite temperature T, as in Ref [2]. In order to compare $YBa_2Cu_2O_{7-\delta}$ (YBCO) with BSCCO, we choose two sets of parameters. For a YBCO model, T_c = 90 K, the penetration depth $\lambda_{ab}(0)$ = 2000 Å, the coherence length $\xi_{ab}(0)$=12 Å, and the effective mass anisotropy $\gamma = \sqrt{M_c/M_{ab}} = 7$. For a BSCCO model, T_c = 84 K, $\lambda_{ab}(0)$ = 2000 Å, $\xi_{ab}(0)$=10 Å, and γ = 100. We also set N_v = 16 and N_z = 40 . The PD is modeled[3] by a cylindrical potential well with a radius $c_0 = \xi_{ab}(0)$ and depth $U_0(T) = (\epsilon_0 d/2)\ln[1+(c_0/\sqrt{2}\xi_{ab}(T))^2]$. We used four random pin configurations for the sample average with the density of pins by 1.05 $\times 10^{12}$ for YBCO and 7 $\times 10^{11}$/cm^2 for BSCCO.

Figure 1 displays calculated vortex phase diagrams for YBCO (a) and BSCCO model (b). In spite of changing anisotropy, three phases (VG, BG, and PG) appear in both two phase diagrams. These three phase components can be thought intrinsic to PDs, whereas the phase boundaries are sensitive to anisotropy. Although the highly anisotropic case γ = 100 shows an almost vertical depinning line T_{dp} (cross) dividing the vortex solid phase into two phases, which was determined by a sharp change in slope of the T-dependence of the in-plane vortex fluctuation $\Delta r_{xy} = \langle |r_{i,z} - r_{i,z}^{\rm ave}|^2 \rangle_{i,z}^{1/2}/a_0$ ($a_0 = \sqrt{\Phi_0/B}$) and depinned vortex fraction $1 - p_{trap}$ (p_{trap} is the trapping rate of the vortices to PDs)[2],

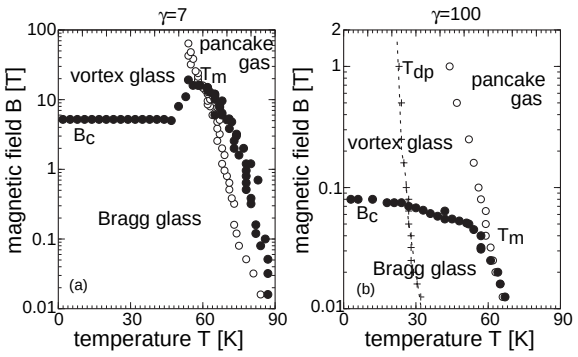

Fig. 1. Calculated vortex phase diagrams: (a) a YBCO model. (b) a BSCCO model.

T_{dp} dose not appear in the case of $\gamma = 7$. In the less anisotropic model, $1-p_{trap}$ takes a value $\simeq 0.64$ even in the strongly pinned regime at very low field $B = 0.016$ [T] and at low temperature T= 2K. In other word, more than half of the vortices in the system are depinned at any time. This suggests that the effect of the elementary pinning are not dominant in the YBCO model in contrast to in the BSCCO model.

The boundary of the BG regime (solid circle) was determined by the criteria $I_{G1} \geq 0.1$. In this BG regime, Δr_{xy} takes the value below 0.25, satisfying the empirical Lindemann criteria. The BG regime becomes expand up to 5 [T] for the less anisotropy case of $\gamma = 7$. It is notable that the BG phase enter into the VG phase up to about 14 [T] at higher temperatures, suggesting recovery of the inplane triangular order because of thermal weakening of pinning. The T_m-line (open circle) was obtained from the sharp change in slope of the T-dependence of the c-axis vortex fluctuation $\Delta r_{zz} = \langle |r_{i,z} - \langle r_{i,z}^{\rm ave} \rangle_z|^2 \rangle_{i,z}^{1/2} / a_0$, as shown in Fig. 2 (c) and (d), distinguishing from the phase of the complete loss of the c-axis coherence. Our obtained phase diagrams agrees with the experimentally obtained phase diagrams[4,5].

Figure 2 shows the T-dependent behavior of I_{G1} (a),(b) and Δr_{zz} (c),(d) for various field B at γ =7 and 100. At low fields G_1 keeps constant value below T_m for the case of $\gamma = 7$, whereas G_1 becomes unstable above T_{dp} at $\gamma = 7$ due to depinning. This difference is expected to come from the two-dimensional fluctuation due to anisotropy. In this regime where I_{G1} survives, as is shown in Fig. 2 (c),(d), Δr_{zz} displays an almost constant behavior, suggesting the c-axis vortex ordering in the BG phase. Δr_{zz} at $\gamma = 7$ takes an value much less than that at $\gamma = 100$, showing the highly-ordered interlayer-coherence at $\gamma = 7$. Through the stronger interlayer vortex-coherence due to less anisotropy, the effect of a trapped vortices is thought to spread over the other layers and to reduce thermal fluctuations, thus the stable phase appears.

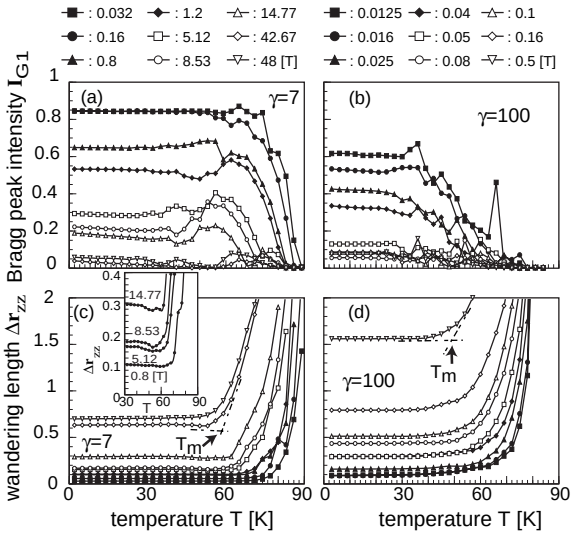

Fig. 2. the T-dependent behavior: The first Bragg peak intensity I_{G1} at γ =7(a), and 100(b). The c-axis vortex fluctuation at γ =7(c), and 100(d). The inset is a magnified part of (c).

As B increases, I_{G1} decreases and tend to almost vanishes in the VG regime. One remarkable thing is that I_{G1} displays a peak structure just below T_m in the intermediate field regime $0.8 \leq B \leq 14.77$ [T] for the case of $\gamma = 7$. The behaviors of Δr_{zz} for some typical fields in this temperature region are magnified in the insert of Fig. 2 (c). We can see the instantaneous decrease just below T_m, implying the reordering of the c-axis coherence. Because of thermal weakening of the effective pinning, the simultaneous recovering of both inter- and intra-layer vortex order appears just below T_m. This regime corresponds to the thermal recovery region in the phase diagram. Therefore the Bragg- or vortex glass phase at low temperatures melts into the pancake gas phase via weakly-pinned glass phase in the presence of dense PDs, whereas the pinning mechanism in the YBCO model is different from that in the BSCCO model which the elementary pinning effect is dominant.

This work was supported by Joint Research Promotion System on Computational Science and Technology (Science and Technology Agency, Japan).

References

[1] G. W. Crabtree and D. R. Nelson, Physics Today (April, 1997) 38.

[2] R. Sugano *et al.*, Physica C (2001) 428.

[3] D. R. Nelson and V. M. Vinokur, Phys. Rev. Lett. **68**, 2398 (1992); Phys. Rev. B **48**, 13060 (1993).

[4] D. T. Fuchs, *et al.*, Phys. Rev. Lett. 80 (1998) 4971.

[5] T. Nishizaki *et al.*, Phys. Rev. B 61 (2000) 3649; Phys. Rev. B 58 (1998) 11169.